

Hydrate Crystals of Alkali Metal-Chloranil and -Bromanil Salts and Their Optical and Magnetic Properties

Shoji HIROMA and Haruo KURODA

Department of Chemistry, Faculty of Science, The University of Tokyo, Hongo, Bunkyo-ku, Tokyo 113

(Received August 28, 1974)

The potassium-chloranil ($K^+ \cdot CA^-$), sodium-chloranil ($Na^+ \cdot CA^-$) and sodium-bromanil ($Na^+ \cdot BA^-$) salts were found to form hydrates when their crystalline powders are exposed to a humid air. In the single crystal spectrum of $K^+ \cdot CA^-$, the charge-transfer band significantly increased its intensity on hydration, exhibiting the same polarization as in the spectrum of the water-free state. It was concluded that CA^- ions in the hydrate crystal are closely stacked on each other to form columns as in the water-free crystal and the charge transfer interaction between CA^- ions is stronger in the hydrate crystal than in the water-free crystal. The spin concentration of $K^+ \cdot CA^-$ markedly decreased on hydration, it being 2.2×10^{22} spins per mol in the state of hydrate while 5.5×10^{23} spins per mol in the water-free state. The hydration resulted in an increase of the intensity of charge-transfer band and a decrease of the spin concentration also in the cases of $Na^+ \cdot CA^-$ and $Na^+ \cdot BA^-$. It is also shown that organic solvents such as acetone, methy ethyl ketone and dichloromethane can enter into the crystal lattice of $K^+ \cdot CA^-$ to form the solvent-containing crystals.

The potassium-chloranil salt, $K^+ \cdot CA^-$, has been reported¹⁾ to exhibit a phase transition in the temperature range, 210—270 K, where it changes from the low spin state to the high spin state. Since this type of phase transition is of general interest in connection with the electronic behaviors of organic radical salts, we investigated the changes of the electronic spectrum of the $K^+ \cdot CA^-$ crystal below and above the transition point by means of a microspectrophotometer equipped with a cryostat at the sample stage.²⁾ In the course of this investigation, we found that, at the room temperature, the crystal spectrum appreciably changed on pumping out the air from the cryostat, but the original spectrum was recovered when the atmospheric air was introduced. We have concluded that the above spectral change takes place because the $K^+ \cdot CA^-$ crystal absorbs water to be a hydrate when kept in the atmospheric air, but this hydrate easily loses water molecules when kept in vacuum.

In the solution, the chloranil anion is known to be quite unstable in the presence of water. In effect, we need to exclude water thoroughly from the solvent which is used in synthesizing the $K^+ \cdot CA^-$ salt. Therefore it has been generally believed that the $K^+ \cdot CA^-$ salt decomposes when exposed to a humid air. However, we found that this is not necessarily the case. The $K^+ \cdot CA^-$ salt does not decompose, but forms a hydrate in a humid air. We found also that the sodium-chloranil, $Na^+ \cdot CA^-$, and sodium-bromanil, $Na^+ \cdot BA^-$, have a much strong tendency to form hydrates when exposed to the atmospheric air, which are again not very much unstable. It was recently reported also by Tsuda *et al.* that the powder of $Na^+ \cdot CA^-$, obtained by the ordinary procedures of preparation, was in the state of hydrate.³⁾

In the present paper, we will report the experimental evidences for the formation of the hydrates of $K^+ \cdot CA^-$, $Na^+ \cdot CA^-$ and $Na^+ \cdot BA^-$, and discuss some of the electronic properties of these hydrates.

Experimental

The crystalline powders of $K^+ \cdot CA^-$, $K^+ \cdot BA^-$, $Na^+ \cdot CA^-$ and $Na^+ \cdot BA^-$ were prepared according to the procedures

reported by Torrey and Hunter,⁴⁾ by using acetone as the solvent. The water-free powders of these salts were obtained by drying the salt powders over phosphorus pentoxide in a vacuum desiccator (at about 10^{-3} Torr). The powder specimens of various water contents were obtained by exposing the synthesized powders of the salts to the air, with or without controlling the humidity, for different lengths of time.

The X-ray powder diffraction patterns were obtained with an automatic recording X-ray diffractometer, Geigerflex (Rigaku Denki), employing CuK_α radiation.

We carried out the differential thermal analysis (DTA) or differential scanning calorimetry (DSC) simultaneously with the thermogravimetric analysis (TGA) by means of a Rigaku TG-DTA (DSC) apparatus with the heating rate, $2.5^\circ C/min$. The powders of KNO_3 and NH_4NO_3 were used as the reference for determining the enthalpy change corresponding to an endothermic peak of a DTA (or DSC) curve.

The polarized absorption spectra of single crystals, in the wave number region from 8000 cm^{-1} to 38000 cm^{-1} , were measured with a microspectrophotometer, a modification of Olympus MSP-IV equipped with a cryostat at the sample stage.⁵⁾ The sample crystals of microscopic size were mounted on a thin quartz plate, and placed in the cryostat.

The ESR absorptions of the powder samples were measured at the room temperature with a JEOL-ME spectrometer (at 9.4 GHz). The spin concentration was determined from the integrated intensity by using DPPH as the reference.

The infrared spectra of the powder samples were measured by means of the Nujol mull method.

Results and Discussion

Characterization of the Hydrates. The infrared spectrum of the powder of $K^+ \cdot CA^-$ was found to vary depending on the treatment after the synthesis. The infrared spectra of the two typical cases are compared in Fig. 1(a): the spectrum I was obtained when the salt powder had been kept in the atmospheric air for a few hours after the synthesis, and the spectrum II was obtained when it had been dried in a vacuum desiccator containing silica gel as the desiccating agent. The spectrum I shows absorption bands at 3400 , 1630 , 1000 cm^{-1} whereas these bands are missing in the spectrum II, and, at the same time, other bands of the former spectrum are a little shifted as compared with

the corresponding bands of the latter spectrum.

The infrared spectrum of $\text{K}^+\cdot\text{CA}^-$ was previously studied by Iida⁶⁾ and by Girlando *et al.*⁷⁾ The spectrum II of Fig. 1(a) coincides with the results reported by these authors, and all absorption bands in this spectrum are assignable to the vibrational modes due to the CA^- ion. On the other hand, the 3400, 1630 and 1000 cm^{-1} bands of the spectrum I can be attributed neither to the CA^- ion nor to the neutral molecule of chloranil. It is also hard to find any chemical species that could be responsible for these bands among the possible decomposition products of the CA^- ion. The above bands disappeared when the powder that had given the spectrum I, was dried in a vacuum desiccator. Conversely, the corresponding bands appeared when we exposed the powder that had given the spectrum II, to the atmospheric air for a few hours. The processes described above were confirmed to be well reversible, and, as we will describe later, we concluded that the spectrum I corresponds to the water-containing state of $\text{K}^+\cdot\text{CA}^-$ while the spectrum II to the water-free state.

A similar change of infrared spectrum was observed on the $\text{Na}^+\cdot\text{CA}^-$ salt. The infrared spectrum of the $\text{Na}^+\cdot\text{CA}^-$ powder which had been kept in the atmospheric air, is shown in Fig. 1(b) as the spectrum I.⁸⁾ This is very much similar to the spectrum of the water-containing powder of $\text{K}^+\cdot\text{CA}^-$ (spectrum I of Fig. 1(a)), exhibiting absorption bands at 3400, 1630, and 1000 cm^{-1} . In this case, however, the above three bands did not disappear even if we kept the powder in a vacuum desiccator for a week with silica gel, although their intensities were reduced to some extent after the above treatment. The spectrum II of Fig. 1(b) is

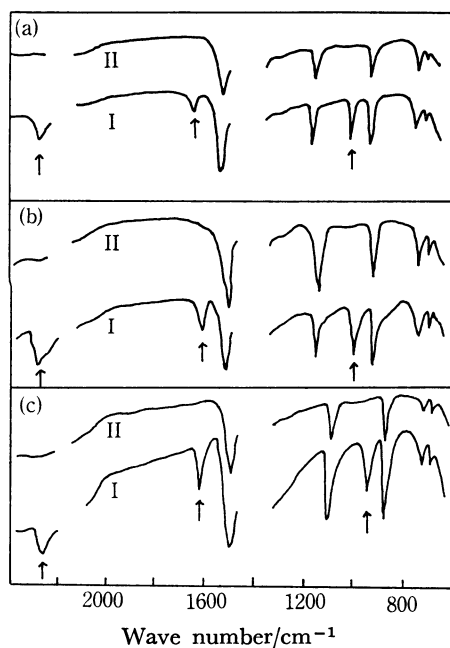


Fig. 1. Infrared spectra of the water-containing states (I) and the water-free states of the salts: (a) $\text{K}^+\cdot\text{CA}^-$, (b) $\text{Na}^+\cdot\text{CA}^-$ and (c) $\text{Na}^+\cdot\text{BA}^-$. The bands characteristic of the water-containing state are indicated with arrows.

the one obtained of the powder that had been heated to 120 °C in the ordinary atmosphere. The same spectrum was obtained with a sample which had been dried well over phosphorus pentoxide. These spectra are free from the 3400, 1630 and 1000 cm^{-1} bands, and almost the same as the infrared spectrum of the water-free powder of $\text{K}^+\cdot\text{CA}^-$.

In Fig. 1(c), we show the spectrum of the $\text{Na}^+\cdot\text{BA}^-$ powder which had been kept in the atmospheric air (spectrum I), and that of the powder which had been heated to 120 °C (spectrum II).⁹⁾ As we compare these two spectra, we can see that the former exhibits absorption bands at 3400, 1630 and 940 cm^{-1} while these bands can not be found in the latter. We can consider that the former is the spectrum of the water-containing state of $\text{Na}^+\cdot\text{BA}^-$. Interestingly, no indication of the formation of the water-containing state was found in the case of $\text{K}^+\cdot\text{BA}^-$. The $\text{K}^+\cdot\text{BA}^-$ powder always gave a spectrum nearly the same as that of the water-free powder of $\text{Na}^+\cdot\text{BA}^-$. The observed spectrum was in good agreement with the spectrum of the $\text{K}^+\cdot\text{BA}^-$ salt reported by Iida,¹⁰⁾ who showed that all observed bands are assignable to the vibrational modes of the BA^- ion.

As we have shown above, the infrared spectrum of the water-containing state is characterized by the presence of the three bands, at 3400, 1630 and 1000 cm^{-1} in the case of $\text{K}^+\cdot\text{CA}^-$ and $\text{Na}^+\cdot\text{CA}^-$ and at 3400, 1630 and 940 cm^{-1} in the case of $\text{Na}^+\cdot\text{BA}^-$. Seemingly it is most reasonable to attribute these bands to the water molecules contained in the salt crystals. A free water molecule is known to have three vibrational modes: the symmetric and antisymmetric stretching vibrations, at 3657 and 3756 cm^{-1} respectively, and the H-O-H bending vibration at 1595 cm^{-1} . Naturally, the infrared absorption bands associated with these vibrational modes are broadened and shifted when the water molecule is contained in the crystal lattice of a salt. In effect, it was reported that the crystals of inorganic hydrates usually show a broad infrared absorption band in the 3000–3500 cm^{-1} region, due to the O-H stretching vibration of water, and one in the 1600–1650 cm^{-1} region, due to the H-O-H bending vibration.¹¹⁾ Therefore we can attribute the 3400

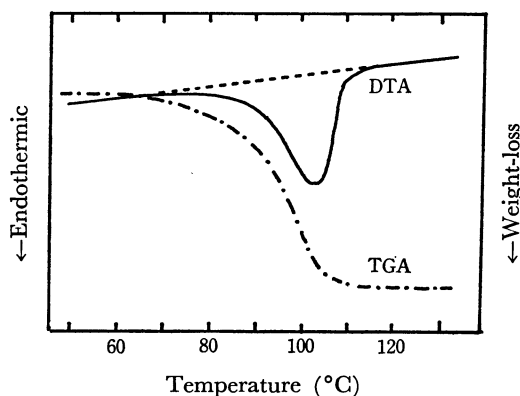


Fig. 2. Differential thermal analysis (DTA) curve and thermogravimetric analysis (TGA) curve of the $\text{Na}^+\cdot\text{BA}^-$ powder which has been exposed to the atmospheric air.

and 1630 cm^{-1} bands which are commonly found in the infrared spectra of the water-containing powders of $\text{K}^+\cdot\text{CA}^-$, $\text{Na}^+\cdot\text{CA}^-$ and $\text{Na}^+\cdot\text{BA}^-$, to the O-H stretching and H-O-H bending vibrations of water. There remains a question as regards the origin of the band at about 1000 cm^{-1} . In this connection, it is interesting to see that inorganic hydrates often exhibit infrared absorption bands in the 800–1000 cm^{-1} region, and these bands have been attributed to the librational motion of water molecule in the crystal lattice.¹¹⁾ Presumably the 1000 cm^{-1} (or 940 cm^{-1}) bands of the present salts can be attributed to the same origin.

We have reproduced in Fig. 2 the DTA and TGA curves obtained of the $\text{Na}^+\cdot\text{BA}^-$ powder which had been kept in the atmospheric air. The DTA curve exhibits an endothermic peak in the temperature region, 67–102 $^{\circ}\text{C}$, where the TGA curve indicates that a weight loss is taking place. By means of the gas chromatography, we examined the chemical species coming out from the powder in the above endothermic process, and were able to confirm that it was entirely composed of water vapor. Similar results were obtained on the air-exposed powders of $\text{K}^+\cdot\text{CA}^-$ and $\text{Na}^+\cdot\text{CA}^-$, although the height and temperature range of the endothermic peak were different for different salts.

From the DTA-TGA (or DSC-TGA) experiments, we simultaneously determined for each powder sample enthalpy of dehydration and the amount of water per one mol of the salt. These values varied depending on the humidity of the atmosphere in which the powder had been kept and on the time length of keeping the powder in such an atmosphere. The mole ratio of water salt, found for the two typical conditions, are shown in Table 1, where "the normal state" means that the sample powder had been kept for one week in a vacuum desiccator (at about 10^{-3} Torr) containing silica gel, and "the highly-hydrated state" means that the sample powder had been exposed for two days to the air saturated with water vapor at the room temperature. Seemingly the latter corresponds to the state of the maximum water content. It is to be noted that the maximum water mole ratio is more than 6 in the case of $\text{Na}^+\cdot\text{BA}^-$ whereas it seems to be about 3 in the cases of $\text{K}^+\cdot\text{CA}^-$ and $\text{Na}^+\cdot\text{CA}^-$.

In Figures 3(a)–(c), we have plotted the enthalpy of dehydration ΔH per one mol of the salt, against the water mol ratio, n . In the $\text{K}^+\cdot\text{CA}^-$ salt, ΔH is proportional to n up to $n=2$, but ceases to increase when $n>2$. This relation between ΔH and n , suggests that there are some changes as regards the state of

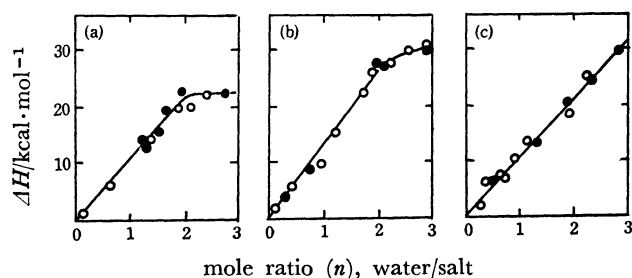


Fig. 3. Relation between the enthalpy of dehydration ΔH (per one mol of salt), and the water mole ratio n ; (a) $\text{K}^+\cdot\text{CA}^-$, (b) $\text{Na}^+\cdot\text{CA}^-$ and (c) $\text{Na}^+\cdot\text{BA}^-$. Solid circles are from differential scanning calorimetry and open circles from differential thermal analysis.

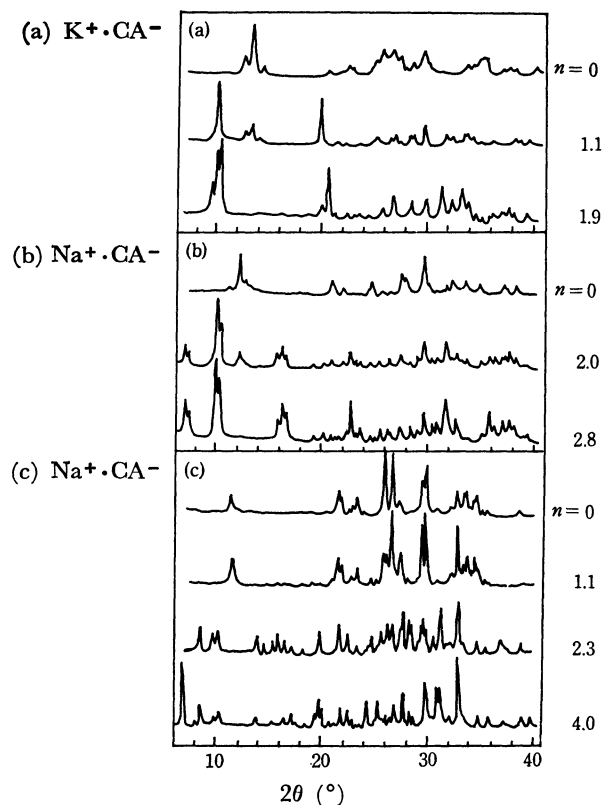


Fig. 4. X-ray diffraction patterns of the salt powders of different water mole ratios; (a) $\text{K}^+\cdot\text{CA}^-$, (b) $\text{Na}^+\cdot\text{CA}^-$ and (c) $\text{Na}^+\cdot\text{BA}^-$. The value of water mole ratio is indicated at the right of each diffraction pattern.

water molecules in the salt crystals when the water mole ratio exceeds 2. A similar relation between ΔH and n was observed on $\text{Na}^+\cdot\text{CA}^-$, in which, although the slope of the ΔH vs. n curve changes at about $n=2$, ΔH is still increasing with a further increase of the water content. The enthalpy of dehydration per one mol of water corresponding to the initial linear region of the ΔH vs. n plot, was estimated as 11.0 and 14.0 kcal/mol for $\text{K}^+\cdot\text{CA}^-$ and $\text{Na}^+\cdot\text{CA}^-$ respectively.

The ΔH vs. n plot of the $\text{Na}^+\cdot\text{BA}^-$ salt is significantly different from the above two salts. In this case, ΔH was found to be proportional to n in a wider range of water content, with the enthalpy of dehydration per one mol of water, 13.3 kcal/mol.

TABLE 1. AMOUNT OF WATER CONTAINED IN THE POWDER SAMPLES

Salt	Water mole ratio (water/salt)	
	Normal state ^{a)}	Highly-hydrated state ^{a)}
$\text{K}^+\cdot\text{CA}^-$	0	2.8
$\text{Na}^+\cdot\text{CA}^-$	2.0	3.1
$\text{Na}^+\cdot\text{BA}^-$	1.3	6.2

a) see text.

The X-ray powder diffraction patterns of the three salts at different water contents are reproduced in Fig. 4. Konno *et al.*¹²⁾ reported that there are two modifications of the $K^+ \cdot CA^-$ salts, α - and β -form, at the room temperature, and carried out the crystal structure analysis on the α -form crystal. By comparing with the crystal data reported by these authors, we were able to conclude that the X-ray powder diffraction pattern of the water-free sample shown in Fig. 4(a), is the one due to the α -form crystals. According to the reported crystal structure of the α -form crystal, CA^- ions are stacked on each other with equal intervals to form columns parallel to the c axis, and such CA^- columns are mutually held together through K^+ ions without leaving such a space that can accommodate water molecules. Therefore, a considerable change must take place in the crystal structure in order to accommodate water molecules in the crystal lattice to form a hydrate crystal. In effect new peaks were observed in the diffraction patterns of water-containing samples. When the water mole ratio was in the range $0 < n < 2$, the diffraction pattern was consisting of the peaks due to the hydrate crystals and those due to the water-free crystals, and the relative intensities of the former peaks increased on increasing the water mole ratio. The above change in the powder diffraction pattern implies that the water molecules are not distributed uniformly among the crystals in the powder, but the powder is, in reality, a mixture of the water-free crystals and the hydrate crystals. Thus the observed water mole ratio of a powder sample should be interpreted as the average value over such an heterogeneous system.

When the water mole ratio of the $K^+ \cdot CA^-$ powder is about 2 or higher, the powder diffraction pattern shows peaks different from those of the hydrate crystals mentioned above (see the diffraction pattern of the sample with $n=1.9$ in Fig. 4(a)). These peaks are likely to be due to another type of hydrate with a higher water content. We will tentatively call this as hydrate II and the other as hydrate I. The powder diffraction patterns indicated that the powders of the water mole ratios, $2 < n < 3$, are composed of the crystals of hydrate I and hydrate II, and the latter content increases with the increase of the water mole ratio of the powder. As we compare the change in the powder diffraction pattern and the relation between ΔH and n shown in Fig. 3, it is most likely that hydrate I has the water mole ratio of approximately 2, and hydrate II a value higher than that, possibly about 3.

The water-containing samples of $Na^+ \cdot CA^-$ showed the X-ray diffraction patterns which consisted of the peaks due to the water-free crystals and those due to the hydrate crystals. With the increase of the water mole ratio of the powder, the former peaks decreased their intensities, but did not disappear until the water mole ratio exceeded 2.5. We noted also that the position of the diffraction peaks of the hydrate crystal little changed throughout the studied region of the water mole ratio, while their intensities relative to each other varied a little depending on the water content. These facts seem to suggest that the hydrate crystal

formed in the initial stage of hydration has a composition corresponding to the water mole ratio higher than 2, and its structure has a space to accommodate more water molecules without causing a significant change in the skeleton of the crystal structure.

The behavior of the $Na^+ \cdot BA^-$ salt was found to be markedly different from those of the above two salts. The diffraction pattern of the powder sample of which water mole ratio was 1.1, was not very much different from that of the water-free sample (see Fig. 4(c)). This seems to indicate that, in the first stage of hydration, water molecules can enter into the lattice of the water-free crystal of $Na^+ \cdot BA^-$ without any significant change of the crystal structure. The second stage of hydration was found to take place as the water mole ratio of the powder was about 2, where new peaks started to appear in the powder diffraction pattern. Another type of diffraction pattern was observed with the samples of a higher water mole ratio. Thus we can presume that there are three or more different stages of hydration in the case of $Na^+ \cdot BA^-$.

Crystal Spectra of the Hydrates. We studied the effects of hydration on the electronic spectra of the single crystals of the salts using a microspectrophotometer equipped with a cryostat at the sample stage of the microscope system of the spectrometer. We used the cryostat as the sample cell for the purpose to control the ambient atmosphere and temperature of the sample crystal. On each salt, we first measured the absorption

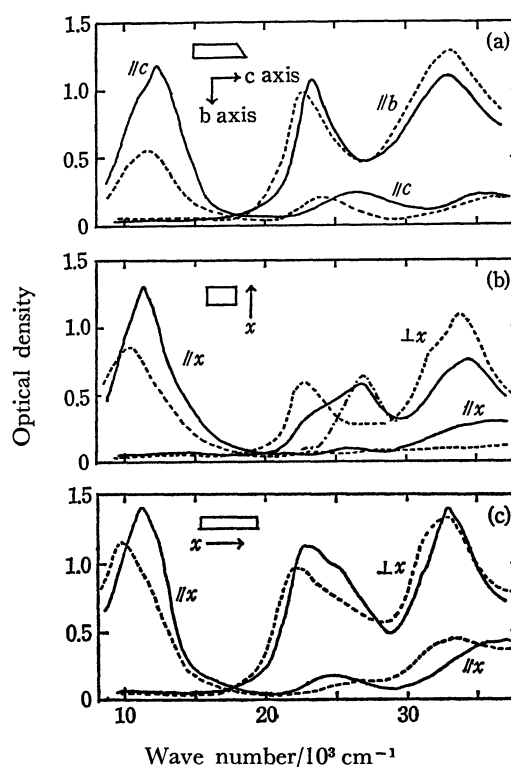


Fig. 5. Polarized absorption spectra of single crystals of $K^+ \cdot CA^-$ (a), $Na^+ \cdot CA^-$ (b) and $Na^+ \cdot BA^-$ (c): — hydrated state, --- water-free state. (The lowest ${}^2B_{1u} \leftarrow {}^2B_{2g}$ band observed at a highly-hydrated state of the $Na^+ \cdot CA^-$ crystal is indicated in Fig. 5 (b) with — · — · —)

spectrum of the sample crystal in the atmospheric air, then pumped out the air from the sample cell and, if necessary, heated the crystal to about 100 °C for a short while, and then measured again the absorption spectrum at the room temperature without breaking the vacuum of the sample cell.¹³⁾ The results of such experiments are shown in Fig. 5. Unfortunately there was no way to know the water content of the sample crystal at the condition of the spectral measurement, but we can consider that, in each case, the sample crystal was originally in the state of hydrate with the water mole ratio of about 2,¹⁴⁾ and was converted to the water-free state by the treatment given within the sample cell of the spectrometer.

In the case of the $K^+ \cdot CA^-$ salt, the crystal changed to the water-free state without any heat-treatment as soon as the air was pumped out from the sample cell, and the reverse change to the hydrate took place as the atmospheric air was introduced into the sample cell. In our previous paper,²⁾ we discussed the assignment of each absorption band of the spectrum of the water-free crystal, and attributed the 11.5×10^3 cm^{-1} band of the c -axis spectrum to the charge transfer between CA^- ions, the 24.0×10^3 cm^{-1} band of the same spectrum to the lowest ${}^2A_u \leftarrow {}^2B_{2g}$ transition of the CA^- ion, and the 23.1×10^3 and 32.7×10^3 cm^{-1} bands of the b -axis spectrum to the lowest and next ${}^2B_{1u} \leftarrow {}^2B_{2g}$ transitions of the CA^- ion, respectively.

The most prominent difference between the hydrate form and the water-free form was found in the region of the charge-transfer band, where the intensity decreased as the crystal changed from the hydrate form to the water-free form, and increased in the reverse process. The differences were less prominent in the region of local excitation bands. However, as compared with the spectrum of the water-free form, the first band of the b -axis spectrum of the hydrate was shifted to higher energy by about 500 cm^{-1} with a little increase of intensity, while the second band of the same spectrum remained at the same position with a little decrease of intensity, and, in the c -axis spectrum, the band due to the ${}^2A_u \leftarrow {}^2B_{2g}$ transition was shifted to higher energy by about 1200 cm^{-1} .

The above-described features of the spectrum of the hydrate resemble in all respects those of the crystal spectrum of the low-temperature phase of the water-free form. We can derive several conclusions concerning the hydrate crystal from these results. First of all, we can conclude that, like in the water-free crystal, CA^- ions in the hydrate crystal must be closely stacked on each other to form the CA^- columns parallel to the crystal axis corresponding to the c axis of the water-free state. Second, we can conclude that the interaction between the neighboring CA^- ions in such a column, is much stronger in the hydrate than in the high temperature phase of the water-free form. This means either that the intervals of CA^- ions in the column have uniformly decreased from those in the water-free crystal or that the CA^- ions are taking a dimeric arrangement in the CA^- columns of the hydrate crystal. Presumably, in the hydrate crystal, the separation between CA^- columns is larger than

in the water-free crystal, so that water molecules are located in the space thus produced between the columns.¹⁵⁾

The crystal structure analysis has not yet been carried out on the $Na^+ \cdot CA^-$ salt. We observed the spectrum for the two polarizations, parallel and perpendicular, respectively, to the x axis that is illustrated in Fig. 5(b). In this case, we needed to heat the sample crystal for a short while to about 100 °C in the vacuum of the sample cell in order to convert the hydrate to the water-free state. The spectra of the water-free state thus obtained resembled the spectra of the water-free crystal of $K^+ \cdot CA^-$. Consequently, the first absorption band, at 10.3×10^3 cm^{-1} , completely polarized in the x direction, can be assigned to the charge transfer band, and the 22.7×10^3 and 33.8×10^3 cm^{-1} bands of the $\perp x$ spectrum to the local excitation bands associated with the two ${}^2B_{1u} \leftarrow {}^2B_{2g}$ transitions of the CA^- ion. However, we noted that the intensity of the charge-transfer band, relative to those of the local excitation bands, is appreciably higher in the water-free $Na^+ \cdot CA^-$ crystal than in the water-free $K^+ \cdot CA^-$ crystal. Thus we can consider that CA^- ions in the crystal of $Na^+ \cdot CA^-$ are forming columns parallel to the x axis, with the interaction between CA^- ions stronger than in the CA^- column of the $K^+ \cdot CA^-$ crystal.

The hydrate crystal exhibits the charge transfer band stronger than that of the water-free form, with a shift of the band maximum by 1300 cm^{-1} to higher energy. Interestingly, the first band of the $\perp x$ spectrum was significantly different from the corresponding band of the water-free form: it showed a maximum at 26.7×10^3 cm^{-1} together with a shoulder at 23×10^3 cm^{-1} , whereas the maximum was located at 22.7×10^3 cm^{-1} in the spectrum of the water-free state. Furthermore, the 23×10^3 cm^{-1} shoulder disappeared when we increased the humidity of the air in the sample cell (see Fig. 5(b)). It has been reported that the CA^- dimer is formed in the solution, and this dimer exhibits the local excitation band associated with the lowest ${}^2B_{1u} \leftarrow {}^2B_{2g}$ transition, at 26.3×10^3 cm^{-1} , while the corresponding band is located at 23.1×10^3 cm^{-1} in the spectrum of the CA^- monomer.¹⁶⁾ In comparison with the above data the appearance of the 26.7×10^3 cm^{-1} band in the spectrum of the highly-hydrated state is likely to be an indication of the strong interaction between CA^- ions. Possibly, CA^- ions are taking a dimeric arrangement in the CA^- column of the hydrate of $Na^+ \cdot CA^-$.

The spectra of the water-free and hydrate states of $Na^+ \cdot BA^-$ are shown in Fig. 5(c). We observed the spectra for the two polarizations, parallel and perpendicular respectively to the elongated direction of the crystal (the x direction in Fig. 5(c)). In this salt, it was necessary to heat the crystal to about 100 °C to convert it to the water-free state.

The solution spectrum of the BA^- ion exhibits absorption bands at 22.2×10^3 and 30.3×10^3 cm^{-1} respectively (see Fig. 6). These two absorption bands correspond to the two ${}^2B_{1u} \leftarrow {}^2B_{2g}$ bands (at 22.2×10^3 and 31.1×10^3 cm^{-1}) of the solution spectrum of the CA^- ion. Thus we can attribute the two absorption

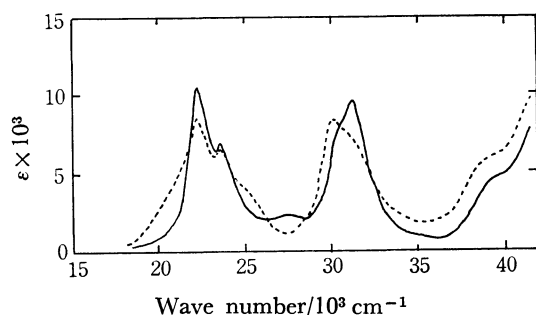


Fig. 6. Absorption spectrum of the CA^- ion (—) and that of the BA^- ion (---) in the acetonitrile solutions of $\text{K}^+\cdot\text{CA}^-$ and $\text{K}^+\cdot\text{BA}^-$, respectively.

bands in the $\perp x$ spectrum of the $\text{Na}^+\cdot\text{BA}^-$ crystal to the local excitations associated with the above two transitions of the BA^- ion, and the near-infrared band in the $\parallel x$ spectrum to the charge-transfer band.

We can consider that, in the crystal of $\text{Na}^+\cdot\text{BA}^-$, BA^- ions are stacked along the crystal axis parallel to the x direction, with a considerably strong interaction between BA^- ions.

As in the cases of other two salts, the charge-transfer band is shifted to higher energy as a result of the hydration, with a little increase of intensity: the maximum is located at $11.3 \times 10^3 \text{ cm}^{-1}$ in the spectrum of the hydrate while it is at $9.6 \times 10^3 \text{ cm}^{-1}$ in the spectrum of the water-free state. Interestingly, the intensity of the charge-transfer band decreased for further increase of the degree of hydration, and the charge-transfer band almost disappeared in the highly-hydrated state.

Spin Concentrations of the Hydrates. All salts studied here showed ESR absorptions due to the anion radicals, CA^- or BA^- , but their intensities were found to be markedly affected by hydration. In Table 2, we listed the observed spin concentrations of the powder samples. The spin concentration was generally higher in the water-free state than in the water-containing state. In particular, a marked difference was found in the case of $\text{K}^+\cdot\text{CA}^-$: the spin concentration of the water-free powder corresponds to almost 90 percent of the theoretical value that is expected when we assign one free spin to each CA^- ion, whereas that of the water-containing state corresponds to only 5 percent of this theoretical value. The latter is nearly the same as the spin concentration of the low temperature phase of the water-free state. In the cases of $\text{Na}^+\cdot\text{CA}^-$ and $\text{Na}^+\cdot\text{BA}^-$, the spin concentration was very low even in the water-free state, but it decreased further in the water-containing state. Interestingly, however, the spin concentration of the $\text{Na}^+\cdot\text{BA}^-$ powder increased again as the water mol ratio exceeded 4, and reached a value of about 5×10^{23} spin per mol at the state of the highest water mole ratio.

If we compare the results described above with the effects of hydration on the crystal spectra, it is quite evident that there is a close correlation between the spin concentration and the intensity of charge-transfer band. In the case of the $\text{K}^+\cdot\text{CA}^-$ salt, the hydration results in an appreciable increase of the intensity of charge-transfer band, which is accompanied by a mark-

TABLE 2. THE SPIN CONCENTRATIONS OF THE POWDER SAMPLES (spins per mol of the salt)

Salt	Water-free state	Water-containing state ^{a)}
$\text{K}^+\cdot\text{CA}^-$	5.5×10^{23}	2.2×10^{22} ($n=1.9$)
$\text{Na}^+\cdot\text{CA}^-$	3.9×10^{22}	2.7×10^{22} ($n=2.0$)
$\text{Na}^+\cdot\text{BA}^-$	6.3×10^{22}	1.0×10^{22} ($n=2.3$)

a) The water mole ratio of the powder sample is given in the parentheses.

ed decrease of spin concentration, and, in the cases of other salts also, the spin concentration is always found to be lower when the intensity of charge-transfer band is higher.

In our previous paper,²⁾ we have shown that the intensity of charge-transfer band of the water-free $\text{K}^+\cdot\text{CA}^-$ crystal increases as the salt changes from the high spin state to the low spin state on lowering the temperature below the transition point, and there is a close correlation between the temperature dependence of spin concentration and that of the intensity of charge-transfer band. We pointed out that the above correlation can be understood in the following way; If we assume a dimeric arrangement of CA^- ions in the CA^- columns of the $\text{K}^+\cdot\text{CA}^-$ crystal of the low temperature phase, there will be a singlet state and a triplet state associated with the interaction between CA^- anion radicals, in which the former state will be a little stabilized in respect to the latter state because of the charge-transfer interaction, consequently, the population of such a singlet state will increase while that of the triplet state will decrease on lowering the temperature, and, since the intensity of charge transfer band is governed by the singlet population whereas the spin concentration is governed by the triplet population, the former increases while the latter decreases as the temperature is lowered.

As we have shown in the preceeding section, the crystal spectra indicate that the charge-transfer interaction between the neighboring CA^- ions in the CA^- columns is much stronger in the hydrated state of the $\text{K}^+\cdot\text{CA}^-$ crystal than in the water-free state. Therefore, we can presume that the singlet state associated with the interaction between CA^- ions has been much stabilized in the hydrate than in the water-free crystal. This must result in the higher singlet population and lower triplet population in the hydrate crystal as compared with the water-free crystal, hence a higher intensity of the charge-transfer band and a lower spin concentration. These are in accord with the observations. Presumably, the same model can be applied for understanding the effects of hydration on the spin concentrations of other salts.

Solvent-containing Forms of $\text{K}^+\cdot\text{CA}^-$. We have confirmed from the infrared spectrum and X-ray powder diffraction pattern that the $\text{K}^+\cdot\text{CA}^-$ powder prepared from the acetone solution is usually not containing solvent molecules. This was also the case when methyl ethyl ketone or dichloromethane was used as the solvent. However, we found that the solvent-containing form of $\text{K}^+\cdot\text{CA}^-$ can be prepared by exposing the salt powder which has been brought to a

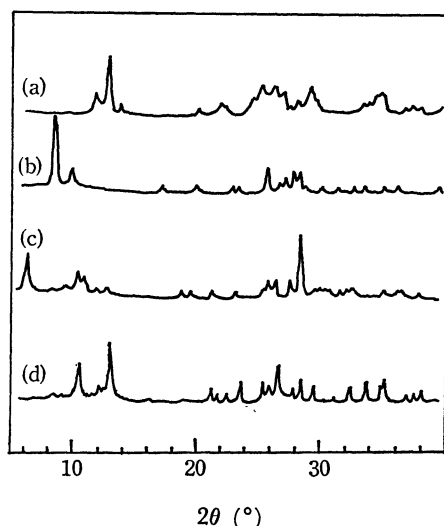


Fig. 7. X-ray diffraction patterns of the solvent-free and solvent-containing powders of $K^+ \cdot CA^-$. (a): Solvent-free, (b): acetone, (c): methyl ethyl ketone, (d): dichloromethane.

nearly water-free state, to the solvent vapor for a sufficiently long period.

The X-ray powder diffraction patterns of such solvent-containing states are shown in Fig. 7, together with the diffraction pattern of the solvent-free state. We can see that the diffraction patterns of the solvent-containing states are different both from that of the water-free state and from those of the hydrates, of which diffraction patterns have been shown in Fig. 4.

In the infrared spectra of the solvent-containing states, we were able to find the bands due to the included solvent molecules: for instance, the bands at 1710 cm^{-1} (C=O stretching) and 1230 cm^{-1} (C-C=O antisymmetric stretching) in the case of acetone, and at 725 and 700 cm^{-1} (C-Cl stretching) in the case of dichloromethane.

The solvent molecules are liberated when we heat the solvent-containing crystals. By means of the DSC-TGA experiment, we determined the amount of the

TABLE 3. PROPERTIES OF THE SOLVENT-CONTAINING STATES OF $K^+ \cdot CA^-$

Solvent	Maximum amount of solvent ^{a)} (mole ratio, solvent/ $K^+ \cdot CA^-$)	Enthalpy of solvent evolution ^{b)} [Kcal/mol of solvent]	Spin concentration [spins/mol of $K^+ \cdot CA^-$]
Acetone	0.90	19	7×10^{21}
Methyl ethyl ketone	0.55	20	3.2×10^{23}
Dichloromethane	0.33	13	2.0×10^{23}

a) The amount of solvent obtained on the powder sample which had been kept for a sufficiently long period in the solvent vapor. b) The value obtained by dividing the value of the enthalpy change corresponding to the endothermic peak of DTA curve, due to the solvent evolution, by the amount of the solvent initially contained in the sample.

solvent contained in the salt, and the enthalpy of solvent evolution. The maximum amount of the included solvent and the enthalpy of solvent evolution per one mol of the solvent are shown in Table 3 together with the observed spin concentration of the solvent-containing powder.

The results described above prove that the solvent molecules do enter into the crystal lattice of $K^+ \cdot CA^-$ to form the solvent-containing forms. At present, we do not know the reason why we did not obtain the solvent-containing crystal on synthesizing the salt from the acetone solution. We noted that the formation of the solvent-containing form becomes rather difficult if we completely remove water from the powder of $K^+ \cdot CA^-$. This might have bearings on the phenomenon mentioned above.

In the visible absorption spectra of the solvent-containing crystals, the charge-transfer band was observed with the same polarization as that of the spectrum of the solvent-free crystal. Therefore we can consider that CA^- columns of the $K^+ \cdot CA^-$ crystal are not destroyed on forming the solvent-containing crystals, and the solvent molecules are likely to be located in the space between CA^- columns.

References and Notes

- 1) J. J. Andre and G. Weil, *C. R. Acad. Sci., Paris, Ser. B*, **266**, 1057 (1968); *ibid.*, **269**, 499 (1969); *Chem. Phys. Lett.*, **9**, 27 (1971).
- 2) S. Hiroma and H. Kuroda, *This Bulletin*, **46**, 3645 (1973).
- 3) M. Tsuda, N. Sakai, I. Shirotani, and K. Murano, *Chem. Lett.*, **1973**, 427.
- 4) H. A. Torrey and W. Hunter, *J. Amer. Chem. Soc.*, **34**, 702 (1912).
- 5) For the details of the spectrometer and the procedures of the measurement, refer to the following paper; H. Kuroda, S. Hiroma, T. Kunii, and H. Akamatu, *J. Mol. Spectrosc.*, **22**, 60 (1967). The sample crystals used for the spectral measurement were typically of the size, a few micron in width and length and less than one micron in thickness.
- 6) Y. Iida, *This Bulletin*, **43**, 345 (1970).
- 7) A. Girlando, H. Morelli, and C. Pecile, *Chem. Phys. Lett.*, **22**, 553 (1973).
- 8) A similar result was reported recently by Tsuda *et al.* (Ref. 3), who reported also the X-ray diffraction pattern of a water-containing powder.
- 9) The powder that had been dried over phosphorus pentoxide showed the same infrared spectrum as the spectrum II.
- 10) Y. Iida, *This Bulletin*, **46**, 2955 (1973).
- 11) R. E. Hester, K. Krishnan, and C. W. J. Scaife, *J. Chem. Phys.*, **49**, 1100 (1968).
- 12) M. Konno, H. Kobayashi, F. Marumo, and Y. Saito, *This Bulletin*, **46**, 1987 (1973).
- 13) The vacuum was in the order of 10^{-5} Torr.
- 14) This was concluded by examining the average water mol ratio of the crystalline powder from which the sample crystals were selected out.
- 15) This seems to be consistent with the observed changes of the X-ray powder diffraction pattern.
- 16) N. Sakai, I. Shirotani, and S. Minomura, *This Bulletin*, **44**, 675 (1971).